Possible role of left–right asymmetry in the sensory system and behavior during adaptation to food-sparse cave environments

Vânia Filipa Lima Fernandes[1], Yannik Glaser[2], Motoko, Iwashita[1], and Masato Yoshizawa[1]

[1] School of Life Sciences, University of Hawai'i at Mānoa, Honolulu, Hawai'i, USA

[2] Department of Information and Computer Sciences, University of Hawai'i at Mānoa, Honolulu, Hawai'i, USA

Corresponding author: Masato Yoshizawa (yoshizaw@hawaii.edu)

Abstract

Laterality in relation to behavior and sensory systems is found commonly in a variety of animal taxa. Despite the advantages conferred by laterality (e.g., the startle response and complex motor activities), little is known about the evolution of laterality and its plasticity in response to ecological demands. In the present study, a comparative study model, the Mexican tetra (*Astyanax mexicanus*), composed of two morphotypes, i.e., riverine surface fish and cave-dwelling cavefish, was used to address the relationship between environment and laterality. The use of a machine learning-based fish posture detection system and sensory ablation revealed that the left cranial lateral line significantly supports one type of foraging behavior, i.e., vibration attraction behavior, in one cave population. Additionally, left–right asymmetric approaches toward a vibrating rod became symmetrical after fasting in one cave population but not in the other populations. Based on these findings, we propose a model explaining how the observed sensory laterality and behavioral shift could help adaptations in terms of the tradeoff in energy gain and loss during foraging according to differences in food availability among caves.

Conflict of Interest: The authors declare no competing financial interests.

Acknowledgement: We thank L Espinasa for constructive comments regarding insights on variation of laterarities in *Astyanax* cavefish. We also thank to H Yoshizawa for supporting the repeatability experiments and fish care assistance. We are grateful to H Hernandez, N Doeden, C Balaan, V Crystal, J Choi, L Lu, J Nguyen, K Lactaoen, M Worsham, J Kato, M Ito, R Balmilero-Unciano, E Doy, A Martinez, and D Mones for fish care assistance. We gratefully acknowledge support from the National Institute of Health (P20GM125508) to MY, Hawaii Community Foundation (18CON-90818) to MY.

Author contribution:

VFLF: designed and performed experiments, wrote original draft, edited the manuscript, performed all experiments, and analyzed results.
YG: designed the detection and analysis algorithm and helped with actual analysis related to DeepLabCut-based aanalysis, consulted the experimental procedure, and edited the manuscript.
MI: performed experiments, edited the manuscript, analyzed the results, and developed a mathematical model.
MY: designed the experiment, edited the manuscript,co-developed DeepLabCut-based analysis method and algorithm, and analyzed the results.

Introduction

Laterality, which is common among various animal taxa, is expressed, for example, as the asymmetrical use of the left or right hand or foot (Tommasi, 2009), the biased use of the left or right eye, and the use of the left or right brain hemispheres for different processing tasks (Heilman and Abell, 1980; Nottebohm, 1977, 1971; Nottebohm and Nottebohm, 1976; Rogers, 1981; Rogers and Workman, 1989; Schwartz et al., 1975; Wernicke, 1874). Laterality confers several advantages in recognizing and escaping from predators (Chivers et al., 2017, 2016; Dadda et al., 2010), facilitating complex and intricate motor activities (Magat and Brown, 2009) and enabling spatial learning (Sovrano et al., 2005). Phylogenetic studies have shown that left–right (L–R) asymmetric traits have repeatedly and independently evolved among different animal taxa (Güntürkün et al., 2020), possibly due to the need for laterality in diverse environments. However, the influence of environments on variation in the laterality and its plasticity among populations has not been well-studied.

As an entry point to solve this evolutionary question, we explored the environment–laterality relationship in *Astyanax mexicanus*, the Mexican tetra, which has two interfertile morphotypes, i.e., surface fish and cavefish (Keene et al., 2016; Protas and Jeffery, 2012; Rétaux et al., 2013; Wilkens et al., 1988) and is known as a model for studying the evolution of behavior. Cavefish, the blind cave-dwelling form of *A. mexicanus*, were separated from their surface-dwelling ancestors about 2,000–20,000 years ago (Fumey et al., 2018; Herman et al., 2018). In total, 32 *A. mexicanus* cave populations have been described in Mexico (Espinasa et al., 2020), and many of these populations have evolved morphological, physiological, and behavioral traits independently, likely via adaptation (Borowsky, 2008; Mitchell et al., 1977; Ornelas-García et al., 2008; Strecker et al., 2012; Wilkens et al., 1988).

One type of laterality has been reported in the Pachón cave population of *A. mexicanus* cavefish, i.e., a preference for using the right-side of the body to detect novel immotile objects in the environment (de Perera et al., 2005). However, it is not yet known which environmental factors determine this type of laterality (unclear ecological relevance) or whether it evolved in a surface fish-like ancestor because such laterality in surface fishes has not been investigated.

In the present study, we investigated a well-characterized type of foraging behavior, vibration attraction behavior (VAB), which is evoked in response to 35–40 Hz vibrations (Yoshizawa et al., 2010) within the range potentially produced by soil crustaceans and percolating water (Lang, 1980; Montgomery and Macdonald, 1987). VAB is evolutionarily enhanced in cavefish, and its advantage was demonstrated as they hunt small prey in the dark (Yoshizawa et al.,

2010). Different degrees of increased VAB levels have been reported in lab cave populations and in the original wild cave populations (Espinasa et al., 2021; Yoshizawa et al., 2010), likely due to differences in ecological factors in these caves. Outside of cave environments, VAB may be detrimental because of nocturnal predators, such as prawn fish (Wilson et al., 2004; Yoshizawa and Jeffery, 2011).

VAB is mediated by the mechanosensory lateral line system, which is composed of sensory units known as superficial neuromasts (SNs) particularly located at the eye orbit and the third infraorbital bone (IO3) (Yoshizawa et al., 2012b, 2010). We reported previously that, despite L–R symmetry in the number of SNs in surface and cave morphs, a positive correlation existed between the number of left SNs and VAB level in Pachón cavefish (Fernandes et al., 2018). This asymmetric sensory usage (hereafter termed “sensory laterality”) was not observed in surface fish, suggesting that this sensory laterality emerged through an evolutionary process that conferred some advantage to fish that colonized cave environments (Fernandes et al., 2018).

In the current study, we investigated the asymmetric L–R responses to a vibrating stimulus in *A. mexicanus* populations. In contrast to the Pachón cavefish, independent cavefish populations from the Los Sabinos and Tinaja caves did not show detectable coupling between the left or right SN and VAB levels, indicating that asymmetric sensory–behavior coupling could be adaptive in the Pachón cave. SN ablation revealed that the left SN in Pachón cavefish indeed regulate the number of approaches (NOA) level variation. In Tinaja cavefish, we found alternative L–R asymmetry in their approaches toward a vibrating rod that did not depend on the number of L–R SNs but was dependent on a fasting condition. Specifically, Tinaja individuals that exhibited asymmetric L–R approaches prior to fasting showed L–R balanced approaches after fasting. Such fasting-dependent L–R plasticity was not detected in the Pachón cavefish or surface fish populations.

Our results indicate that different cave populations of *A. mexicanus* have evolved distinct laterality strategies. Our study also suggests that L–R sensory usage and the L–R asymmetric approach have different underlying mechanisms. Based on these findings, we propose a model that explains the advantages of laterality according to diet availability and energy gain and loss. This model implies that the laterality of Pachón cavefish saves energy most effectively among the studied cave and surface populations and may have allowed Pachón cavefish to adapt successfully to the fluctuating availability of food in the Pachón cave.

Results

Sensory laterality among different cave populations of *A. mexicanus*

In a previous study, we reported a positive correlation between the VAB level and the number of left- but not right-side SNs in Pachón cavefish (Fernandes et al., 2018). This L–R asymmetric association between the number of SNs and VAB likely evolved during the cave adaptation process. However, whether such left SN–VAB coupling exists in other discrete cave populations in the context of convergent/parallel evolution was unclear. Thus, we investigated other VAB-positive cave populations in Tinaja and Los Sabinos (Espinasa et al., 2021; Yoshizawa et al., 2015, 2010) (Figure 1). First, to detect left or right approaches toward a vibrating rod, we developed a method using DeepLabCut (DLC), a machine-learning suite (Mathis et al., 2018; see Materials and Methods), with which we accurately measured the X–Y coordinates of the left and right craniums of fish, which was not possible with a method we developed previously (Yoshizawa et al., 2015, 2010). To validate the new method, we measured the number of approaches toward the vibrating rod (NOA) and the duration around the vibrating rod (DIR) in one surface fish and three cavefish populations (see Materials and Methods). Consistent with previous results (Yoshizawa et al., 2015, 2012a, 2010), Pachón cavefish showed the highest level of VAB in comparison to Los Sabinos and Tinaja cavefish and surface fish, both in terms of NOA and DIR (Figure 1C; Supplementary Table 1), indicating that the new detection method is consistent with the method developed previously (Yoshizawa, 2015; Yoshizawa et al., 2012a, 2010).

We then explored whether an L–R bias existed in the couplings between the number of SNs and NOA or DIR. In the surface population, no correlation was detected between the left SNs and the L–R summed NOA/DIR (i.e., total NOA/DIR) or the right SNs and the total NOA/DIR (Figure 1D; statistics in Supplementary Table 2; all NOA and DIR in Figs. 1 and 2 are L–R summed). In contrast, a positive correlation was found between the left SNs and NOA in the Pachón cave population ($\tau = 0.329$, $P = 0.047$; Figure 1G; Supplementary Table 2) but not between the right SNs and NOA ($\tau = 0.258$, $P = 0.118$; Figure 1G; Supplementary Table 2). This result is also consistent with our previous study (Fernandes et al., 2018); thus, we tested the other cave populations with confidence. Both the Los Sabinos and Tinaja cave populations showed results similar to those of the surface population, i.e., no correlation was detected between the left SNs and NOA/ DIR or between the right SNs and NOA/ DIR (Figure 1E and F; Supplementary Table 2). In summary, our machine-learning-based detection method generated results consistent with our previous studies, showing that the left SN number is

151 coupled with the NOA level in the Pachón cave population. However, this method failed to
152 detect such correlations in other cave populations.
153
154 **Coupling between the left SNs and VAB is based on inputs to the left SNs**
155 To investigate the underlying mechanism of the coupling between the left SNs and VAB, we
156 ablated the SNs on either the left or right-side at the IO3 area in the Pachón cave populations
157 using a well-developed noninvasive method (Yoshizawa et al., 2010). To highlight SN–VAB
158 coupling, we selected VAB-positive individuals [NOA ≥ 6; (Yoshizawa et al., 2010)]. The
159 ablation was confirmed using DASPEI staining after the behavior assay (Figure 2A and B).
160 After ablation, Pachón cavefish individuals with a higher percentage of ablated SNs exhibited
161 lower levels of VAB ($\tau = -0.342$, $P = 0.009$; Figure 2B; Supplementary Table 3). However, the
162 change in VAB was not observed when the right-side SNs were ablated ($\tau = -0.064$, $P =$
163 0.635; Figure 2D; Supplementary Table 3). We also performed SN ablation in surface fish and
164 detected no correlation between NOA and the proportion of ablated SNs on the left or right
165 sides (Figure 2—figure supplement 1; Supplementary Table 3). These results reinforce our
166 previous findings (Fernandes et al., 2018) regarding the significant role of the left-side SNs in
167 the VAB of the Pachón cave population.
168 For DIR (i.e., the time spent located within 1.3 cm of the vibrating rod), no correlation was
169 found with the proportions of left or right ablated SNs in Pachón cavefish (Supplementary
170 Table 3), suggesting a possibility that the NOA and DIR are regulated differently, i.e., in
171 Pachón cavefish, NOA could be mediated by the SNs, whereas DIR could be regulated via
172 non-SN means, such as auditory and/or tactile sensing (see the Discussion).
173 Regarding population averages, for Pachón cavefish, the ablation of the left, right, or left and
174 right SNs induced no detectable changes in NOA or DIR (although the ablation of left-side SNs
175 increased NOA significantly: $V = 74.5$, $P = 0.032$; Figure 2—figure supplement 2;
176 Supplementary Table 4; See also Supplementary file 1—extended result and discussion).
177 In summary, for Pachón cavefish, the left SN number raises NOA but not DIR, and the right
178 SNs were not significantly associated with NOA.
179
180 **Behavioral laterality across different populations of *A. mexicanus***
181 Our results showed that the left SNs promoted VAB in Pachón cavefish, whereas the other
182 populations did not show L–R-biased coupling between the SNs and VAB (i.e., sensory
183 laterality) (Figs. 1 and 2). Given that VAB evolved as a foraging behavior and that diet type and

availability differ among caves [e.g., from decomposed plants to soil or cave-adapted arthropods as well as seasonal flooding (Culver, 1982; Culver and Pipan, 2009; Espinasa et al., 2017; Keene et al., 2016; Mitchell et al., 1977; Yoshizawa et al., 2010; Yoshizawa and Jeffery, 2011)], we hypothesized that alternative forms of laterality in VAB exist in surface and/or cave populations. Thus, we explored two types of L–R bias in VAB (i.e., left/right NOA and left/right DIR; Figure 3A) among the surface population and Pachón, Tinaja, and Los Sabinos cave populations. To quantify the lateral preference of individual fish, the right NOA or DIR was divided by the total NOA or total DIR, respectively (i.e., ratio scores of >0.67 and <0.33 indicate right and left preferences, respectively; Figure 3B and 3C). We measured the L–R biases of NOA and DIR separately because our results indicated that they were likely regulated differently (see the previous section and Discussion). Individuals from each of the cave and surface populations showed a preference for one side or the other while approaching (NOA) and touching the rod (DIR) (Figure 3B and 3C, respectively). This L–R preference in each individual was not repeatable or only fairly repeatable in surface fish and Pachón cavefish when we conducted assays 6 days apart and repeated three times (Table 1) [respective NOA intraclass correlation coefficients (ICCs): $\kappa = 0.0$ (none), $P = 0.48$; $\kappa = 0.39$ (fair), $P = 0.00025$. Respective DIR ICCs: $\kappa = 0.0$ (none), $P = 0.48$; $\kappa = 0.085$ (none), $P = 0.20$]. In contrast, Tinaja cavefish individuals exhibited a moderate level of repeatability in NOA ($\kappa = 0.54$, $P = 0.0021$; repeated three times; Table 1), suggesting that these fish tended to consistently approach the vibrating rod unidirectionally.

Table 1. Intraclass correlation coefficient (ICC) under Cohen's suggestion (Landis and Koch, 1977; Zegers et al., 2010) (N = 3 repeats; N= 22 for surface, N = 9 for Pachón cave and N = 11 for Tinaja cave fish).

Population	Measurement	Average L–R ratio	Statistics	Kappa	P-values
Surface fish	NOA	0.459 ± 0.034	$F_{21,42} = 1.0$	0.0 (none)	0.48
Surface fish	DIR	0.481 ± 0.028	$F_{21,42} = 1.0$	0.0 (none)	0.48
Pachón cavefish	NOA	0.464 ± 0.036	$F_{28,56} = 3.0$	0.39 (fair)	0.00025***
Pachón cavefish	DIR	0.473 ± 0.024	$F_{28,56} = 1.3$	0.085 (none)	0.20
Tinaja cavefish	NOA	0.482 ± 0.052	$F_{10,20} = 4.5$	0.54 (moderate)	0.0021**
Tinaja cavefish	DIR	0.478 ± 0.046	$F_{10,20} = 2.4$	0.32 (fair)	0.043*

As shown in the histograms in Figure 3B and C, there was no detectable bias between the left and right-side NOA ($F_{1,152} = 0.149$, $P = 0.700$) or between the left and right DIR among the populations ($F_{1,152} = 3.378$, $P = 0.068$) (Figure 3—figure supplement 1; Supplementary Table 1). Additionally, there was no detectable bias between the duration of left and right facing

213 outside the 1.3-cm radius around the vibrating rod, suggesting that there was no tendency to
214 face left or right in relation to the vibrating rod from a distance ($F_{3,152}$ = 0.016, P = 0.997;
215 Supplementary Table 1).
216
217 The above results suggested that laterality in SN usage (sensory: Pachón cavefish) and
218 laterality in approaches (behavior: Tinaja cavefish) existed in some *A. mexicanus* populations.
219 Therefore, we investigated whether relationships existed between the lateralities in the number
220 of left or right SNs and left or right NOA or left or right DIR. Detailed correlation analyses were
221 performed in the ablation study. In Pachón cavefish, the ablation ratio of the left SNs mirrored
222 the reduction of left approaches (left NOA), but no correlation was detected between the left
223 SN ablation ratio and the right NOA, the right SN ablation ratio and the left or right NOA, and
224 the left or right SN ablation ratio and the left or right DIR (Supplementary Table 3). Additionally,
225 there was no detectable effect of any left or right SN ablation on the L–R approaches (NOA or
226 DIR) of surface fish. These results indicate that the number of left SNs (inputs) affects the left
227 approaches of Pachón cavefish but not those of surface fish. As in the intact SN condition,
228 there were some positive correlations between the number of L–R SNs and the L–R NOA
229 and/or DIR in surface fish and Pachón cavefish (but not in other cave populations; see
230 Supplementary Table 2). However, the SN–behavior relationship of surface fish in the intact
231 state may not be vital because it was not detected in the ablation study.
232 Collectively, these results indicate that sensory laterality was found only in Pachón cavefish
233 and was associated with left-side approaches. Individuals in the Tinaja cave population but not
234 in the surface or Pachón cave populations showed a moderately consistent preference for left-
235 or right-side approaches, and L–R bias was not detectable at the whole population level.
236
237 **Fasting increased sensory responses and reduced approach laterality**
238 Previous prey-capture experiments indicated that VAB promotes the food capture rate in dark
239 and food-sparse environments (Yoshizawa et al., 2010). VAB plasticity according to the
240 environment has also been suggested (Espinasa et al., 2021). Thus, we hypothesized that
241 fasting induces shifts in laterality. Because younger fish are more sensitive to fasting in
242 general, we used 1-year-old (young adult) surface fish, Pachón cavefish, and Tinaja cavefish
243 rather than the 2–3-years-old (adult) fish used in the earlier experiments (Figs. 1–3).
244 First, we investigated the effect of fasting on sensory laterality (i.e., the number of left or right
245 SNs vs. the total NOA or DIR) among the surface, Pachón, and Tinaja populations. The 6-day

246 fasting reduced the total NOA and total DIR in surface fish but increased the total DIR in Tinaja
247 cavefish (Figure 4A and 4B; Supplementary Table 5); however, no changes were detected in
248 Pachón cavefish (Figure 4A and 4B; Supplementary Table 5). To investigate L–R SN–behavior
249 coupling, we determined the correlations between either the number of left or right SNs and
250 the total NOA after fasting with subtraction of the prefasting NOA (Figure 4C; Supplementry
251 Table 7). Pachón individuals with fewer "left" SNs exhibited a higher increase in total NOA
252 (Figure 4C; Supplementry Table 7). Pachón individuals with fewer "right" SNs showed a higher
253 increase in NOA but not at a significant level (Figure 4C; Supplementry Table 7). Surface fish
254 or Tinaja cavefish did not show fasting-dependent changes in SN–approach coupling (Figure
255 4C; Supplementry Table 7). In summary, fasting yielded different responses in the surface and
256 Pachón populations, i.e., NOA was reduced in surface fish, and Pachón individuals with fewer
257 left SNs showed a higher increase in NOA relative to that of individuals with more left SNs.
258 Second, we studied the effect of fasting on laterality in approaches. The surface and Tinaja
259 populations had more number of younger fishes (1-year-old fish vs. 2–3-years-old fish) that
260 showed L–R-biased approaches in the prefasting condition (NOA; broader standard variations;
261 Figure 5A and 5B). In contrast, Pachón cavefish individuals showed L–R symmetrical NOA
262 with a narrower standard variation than that observed in the surface and Tinaja populations in
263 the prefasting condition (Figure 5A and 5B). After 6 days of food deprivation, the distributions
264 of the L–R preference in surface fish became more uniform for both NOA and DIR (Figure 5A,
265 5B, 5C, and 5D). Interestingly, Tinaja cavefish shifted from a right-biased approach (for both
266 NOA and DIR) to a symmetrical approach in NOA (~0.6 in a bias index; Figure 5C) and a
267 reduced right bias in DIR (Figure 5). Regarding population averages, none of surface fish,
268 Tinaja, or Pachón cavefish individuals showed detectable L–R bias in NOA or DIR in the
269 prefasting or postfasting condition, except DIR in Tinaja cavefish (right bias; Figure 5—figure
270 supplement 1A and 1B), which mirrors the observation in Figure 5A and 5B. Fasting also
271 induces alternative responses among surface fish, Tinaja, and Pachón cavefish individuals;
272 surface fish decreased the overall NOA and DIR after fasting, while Tinaja cavefish increased
273 DIR (Figure 5—figure supplement 1A and 1B). Pachón cavefish did not show detectable
274 changes in the overall NOA and DIR levels.
275 In summary, food deprivation drove behavioral shifts in the surface and Tinaja cave population
276 but not in the Pachón cave population, i.e., surface fish showed reduced VAB, whereas Tinaja
277 cavefish showed increased VAB (Figure 5, and Figure 5—figure supplement 1). Furthermore,

Tinaja cavefish showed a postfasting plastic change in the L–R bias of NOA toward a more L–R symmetric approach (Figure 5, and Figure 5—figure supplement 1).

Discussion

We addressed laterality in sensory–behavior coupling and rod approaches among different populations of *A. mexicanus*. Using a newly developed DLC- and machine learning-based video analysis method, we found the following: (1) only the Pachón cave population showed a bias in SN–VAB coupling, i.e., the left SNs promote VAB, but not detectable in other populations; (2) no L–R bias detected in approaches (NOA) and adherence (DIR) in the surface, Pachón, Tinaja, and Los Sabinos cave populations at the population levels, but some individuals, especially those in the Tinaja cavefish population, repeatedly showed a preference for left or right approaches; and (3) fasting for 6 days reduced the L–R-biased in approaches in the Tinaja cave population, indicating that VAB plasticity is present in this population. Thus, L–R asymmetry in foraging behavior seems to have evolved flexibly under different caves, and our findings provide insights into the evolutionary dynamics of L–R asymmetry under ecological pressure (see below). At the end, we discuss the energy-saving advantage associated with foraging laterality.

Introducing a machine-learning method to assess adaptive foraging behavior

With the aid of a DLC neural network (trained with 807 images), we developed a new video analysis method that achieved a detection accuracy of >99%, which was confirmed using a manual survey of the labeled videos. In comparison with our previously reported method (Yoshizawa et al., 2010), this trained network yielded higher resolution for the approach (NOA) and adherence (DIR) events of VAB, and left or right facing in the direction of the vibrating rod could be monitored. The new method was also confirmed to be consistent with the ImageJ-based method developed previously (Figure 1), which supports the findings of the present study as an expansion of the previous results.

Coupling between the left SNs and NOA but not DIR in Pachón cavefish

Pachón cavefish showed a significant correlation between the number of left SNs and NOA. This coupling was observed repeatedly in different cohorts from different Pachón parents (Fernandes et al., 2018). Furthermore, this sensoory laterality in NOA in Pachón cavefish was confirmed in our ablation experiment, i.e., as more left SNs were ablated, the NOA was

reduced. Notably, a correlation between the left SNs and DIR was not detected in Pachón cavefish. Such variation in sensory–behavior coupling suggests that differences exist in the sensory mechanisms underlying NOA and DIR, i.e., given the correlation between the SNs and NOA and our SN ablation results, NOA in Pachón cavefish is likely enhanced by SNs. Contrastingly, DIR was neither correlated with the number of SNs nor changed after SN ablation, indicating that other sensory systems, e.g., tactile and/or auditory sensors, affect DIR. The auditory inner ear can sense near field particle motion based on the motion lag between the fish body and the otolith (Kalmijn, 1988; Popper and Fay, 2011; Tricas, 2020). Overlapping functions between auditory, lateral line, and tactile senses have been noted but not studied in detail in the context of foraging (e.g., Braun and Sand, 2013; Kohashi et al., 2012). VAB thus emerges as a good model behavior of the modality switch between these three sensory systems because it can be evoked from the far field (>5 m in the field: auditory; see below; Espinasa et al., 2021) and near field (possibly; >1.3 cm: lateral line; <1.3 cm: tactile).

Laterality in cranial morphology and behavior

There are reports of cranial bending in adult Pachón and Tinaja cavefish but not in adult surface fish or younger individuals of the Pachón, Tinaja, and surface populations (Powers et al., 2017). We did not detect left cranial bending in our experimental fish (2–3 cm standard length; 1–3 years old), which excludes the confounding effect of head bending on lateralities in sensory–behavior coupling and approaches to the rod. Other morphological asymmetries have been reported previously, e.g., L–R asymmetry in the suborbital (i.e., infraorbital) bone fragmentations in Pachón and Tinaja cavefish but not in surface fish (Gross et al., 2016); and L–R asymmetry in cranial SN distribution but not the number of SNs, which corresponds to asymmetric bone fragmentation (Gross et al., 2016; Gross and Powers, 2016). In the present study, we investigated the L–R asymmetric “number” but not “distribution” of SNs. It will be interesting to investigate whether the SN distribution pattern plays a role in VAB expression in future studies.

Laterality of approaches at the population and individual levels, and the effect of starvation

In our L–R approach study, there was no detectable left or right bias for NOA and DIR at the population level among the four tested populations (with the exception of 1-year-old Tinaja cavefish). However, some individual fish showed one side bias in NOA and/or DIR, and these

344 asymmetric biases were consistent within each individual. Laterality at the individual level has
345 been largely overlooked (Rogers, 1989); nonetheless, studies in chicks and fish showed that
346 behavior lateralization was random in a population but existed and seemed advantageous
347 (e.g., by minimizing the use of brain resources) at the individual level in complex tasks,
348 including social interactions (Bisazza et al., 2000; Bisazza and Dadda, 2005; Rogers and
349 Workman, 1989). In the current study, we also revealed plastic laterality in a cave population
350 responding to fasting. Because VAB evolved as a foraging behavior under food-limited
351 conditions (Yoshizawa et al., 2010; Yoshizawa and Jeffery, 2011), we propose that cavefish
352 laterality evolved to conserve energy.
353 Many caves in North-eastern Mexico experience 6-months wet and 6-months dry seasons;
354 thus, cavefish experience food-sparse conditions for ~6 months per year (Espinasa et al.,
355 2017). We tested the effect of food deprivation on L–R asymmetry, and removing food intake
356 for 6 days increased both DIR and L–R symmetric NOA in the starvation resistant Tinaja
357 cavefish (Aspiras et al., 2015). The increases in DIR and symmetric NOA could help boost
358 food intake while saving energy (see below). In contrast, the surface fish, which are less
359 tolerant to starvation, showed decreased NOA and DIR, seemingly saving energy in a simpler
360 manner by reducing the number of foraging attempts. The most derived Pachón cave
361 population (Herman et al., 2018) is also starvation resistant but showed a nonsignificant
362 change in symmetric NOA and DIR, perhaps because these cavefish have optimized their
363 foraging under food-sparse conditions over the course of evolution (see below). In the
364 Supplementary file 1—extended results and discussion, we also discuss age-dependent L–R
365 plasticity in Tinaja cavefish (c.f., Figure 3B and C; Figure 5A and B) and the VAB levels of Los
366 Sabinos and Tinaja cavefish.
367

368 **Advantages of laterality in the cave ecosystem**

369 To understand the evolution of laterality and its plasticity in the context of cave ecology, we
370 propose a model that explains the potential advantages of such lateralities and its plasticity in
371 terms of calorie gain and consumption in food-sparse caves (Figure 6). This model assumes
372 that (1) only one side of SNs accounts for VAB evocation and (2) starvation induces L–R
373 symmetric NOA. Based on these assumptions, we hypothesized that sensory laterality and
374 non-L–R-biased (i.e., symmetrical) approaches are beneficial in food-limited environments at
375 the population level due to the tradeoff between calorie gain and calorie use in foraging.

The model, including food/energy gain, energy loss by thrasting, and the change in the total amount of calories gained in a population (= a sum of fish individuals), can be described as the following function:

$\frac{dE}{dt} = E_g - E_c$ (equation 1; Supplementary file 1),

where E represents the total calories/energy of an average fish in a population gained per unit of time t ($E = \sum_{i=1}^{N} E_i$, where i represents each individual fish and E_i represents the total calories each fish gains per unit time), E_g represents the average total calories the population gains from the diet per unit of time, and E_c is the average total calories the population uses during foraging per unit of time.

Food capturing movements are assumed to use more calories, as the fish perform rapid and short turns toward their food, than are used in a typical swimming motion (personal observation). If the energy gain, E_g, is higher than the energy consumption, E_c (eq. 1), the current fish in the population can survive in the given environment. If the opposite is true ($\frac{dE}{dt} < 0$; eq. 1), the number of fish in the population is reduced. We expect that unilateral sensing has an advantage over bilateral sensing in terms of the tradeoff between E_g and E_c.

Depending on two scenarios, i.e., (1) only a unilateral input or (2) the inputs of both sides are accounted for in VAB expression, the probability of sensing the food (p_d) is defined as follows:

$p_d = \begin{cases} \frac{1}{4} & for\ unilateral\ sensing \\ \frac{1}{2} & for\ bilateral\ sensing \end{cases}$ (equation 5; Supplementary file 1; Figure 6B and C).

When a diet is available in a given cell area and two fish exist in the same cell area, two possibilities exist (Figure 6A): (1) in unilateral sensing, only one fish can sense and acquire the diet ($\frac{E_i}{dt} > 0$), whereas the other fish does not evoke VAB, i.e., no calories are lost in the other fish ($\frac{E_{i'}}{dt} = 0$) (Figure 6A and B); (2) in bilateral sensing, the two individuals compete for the diet unit (which only supplies one fish), resulting in one fish capturing the diet and gaining a positive E value ($\frac{E_{i'}}{dt} > 0$) and the other losing calories due to their foraging activity ($\frac{E_{i'}}{dt} < 0$), which results in many fish losing energy in the population (Figure 6C). The total $\frac{E_i}{dt} + \frac{E_{i'}}{dt}$ in unilateral sensing (1) is larger than that in bilateral sensing (2). This example shows that the number of fish reacting to and capturing food will differ in bilateral- or unilateral sensing

405 situations, resulting in differences in E based on E_c in equation 2 (Supplementary file 1): E_c
406 (calories consumed) depends on p_d (eqs. 2, 4, and 5; Supplementary file 1), so the E_c for
407 bilateral sensing is twice as high as that for unilateral sensing (Figure 6C). As shown in Figure
408 6D and E, in a diet-rich environment, the bilateral sensing population has an advantage
409 because its calorie gain is higher than that of the unilateral sensing population. Under food-
410 sparse conditions, the advantage is reversed because the unilateral sensing population
411 maintains $\frac{dE}{dt} > 0$, whereas the bilateral sensing population does not achieve $\frac{dE}{dt} > 0$ because
412 many failed foraging attempts increase E_c (Figure 6D and F). In summary, the unilateral
413 sensing population can survive better than the bilateral sensing population by reducing the
414 number of failed foraging attempts in food-limited conditions. This model suggests that the
415 sensory laterality of Pachón cavefish could be beneficial in food-limited environments.
416 The laterality in approaches (NOA) is defined as a preference for using the left or right-side of
417 the head/body when approaching the vibration source. Our video observations indicated that
418 fish exhibit multiple quick turns against the vibrating rod when they are in its vicinity (within a
419 1.3-cm radius of the rod). We assume that sharp turns cost more calories than typical
420 swimming. We also assume that the fish that use unilateral approaches make steeper turns
421 more often than the fish that use bilateral approaches (Figure 6G). The different levels of
422 calorie consumption in fish using unilateral and bilateral approaches are implemented in the
423 parameter 'a', the coefficient of E_c, i.e., the average calorie consumption per time unit (eq. 2 in
424 Supplementary file 1). Accordingly, the parameter 'a' value of the fish that use unilateral
425 approaches is higher than that of the fish that use bilateral approaches (hatched lines in Figure
426 6H and I; Supplementary file 1). With this setting, under food-rich conditions, the $\frac{dE}{dt}$ values of
427 fish that use either unilateral or bilateral approaches are positive (Figure 6H); thus, both types
428 of fish are expected to survive. In contrast, a population that uses bilateral approaches has a
429 higher chance of survival ($\frac{dE}{dt} > 0$) than a population that uses unilateral approaches in a food-
430 limited environment ($\frac{dE}{dt} < 0$; Figure 6I). Our starvation experiment showed that Tinaja cavefish
431 shifted their approach from unilateral to L–R balanced (Figure 5A and 5C); therefore, these fish
432 seem to adjust their L–R approach depending on food availability.
433 According to our model, Pachón cavefish is the most optimized population as it shows L–R
434 symmetrical approaches (Figure 5A and 5C) as well as left-biased unilateral sensing (Figs. 1
435 and 2). The degree of laterality in Pachón and Tinaja cavefish populations fits well with their
436 ecological conditions where Pachón cavefish experiences seasonal fluctuation of animated

437 diets, crustaceans, which seems to be available more in the ~6-month dry season than in the
438 6-month wet season (Espinasa et al., 2017; Mitchell et al., 1977). In contrast, several Tinaja
439 cave pools receive percolating water most of the time and have thick organic matter covering
440 the bottom, distinct from Pachón cave, and the plastic laterality may be sufficient for adaptation
441 to cave environment (Mitchell et al., 1977). There might be a possibility that Pachón cavefish
442 reside in a more diet-limited condition than Tinaja, yielding further diversified laterality to adapt
443 to cave environment.
444 In summary, laterality in sensory–behavior coupling and symmetrical approaches may have
445 advantages in food-sparse environments and may have promoted adaptation processes in
446 Pachón cave. Over the course of evolution, Tinaja cavefish evolved a plastic foraging strategy
447 according to food availability, whereas Pachón cavefish evolved a robust SN sensory laterality
448 with balanced approaches to vibrating objects. These results represent new insights that help
449 us better understand the evolution of laterality, and they may lead to further insights into the
450 diversification of laterality among animals.
451
452

453 ## Materials and Methods

454 ### *Astyanax mexicanus* husbandry and ethics statement

455 The lab-raised surface fish population used in this study is descended from an original
456 collection from Balmorhea Springs State Park (Texas, USA), whereas the lab-raised cave
457 populations used in this study are descendants of an original collection from Cueva de El
458 Pachón in Tamaulipas collected by Richard Burowski (2009/2011), and collections from
459 Sótano de la Tinaja and Cueva de Los Sabinos in San Luis Potosí, Mexico collected by Bill
460 Jeffery in (2000 - 2001). The adult fish (1–3 years old) used in the experiments were raised in
461 groups of 20–25 individuals in 0.74-L Ziploc containers (S.C. Johnson & Son Inc., Racine, WI,
462 USA) and 1.4-L Zebrafish Aquatic Housing System tanks (Aquaneering Inc., San Diego, CA,
463 USA). Fish were fed twice per day *ad libitum* with live *Artemia salina* larvae (Brine Shrimp
464 Direct, Ogden, UT, USA).
465 All animal procedures were performed under protocol 17-2560 approved by the Institutional
466 Animal Care and Use Committee at the University of Hawai‘i.
467

468 ### Recording VAB

469 VAB assays were performed as described previously by Yoshizawa et al. (2010) and Worsham
470 et al. (2019). Briefly, fish were acclimated for 4–5 days in a cylindrical chamber (10 cm in
471 diameter; 5 cm in height; Pyrex 325 mL; Corning, NY, USA) filled with conditioned water (pH
472 6.8–7.0; conductivity of ~700 μS). Fish were fed once per day *ad libitum* with live *A. salina*
473 larvae. After acclimation, the behavior of fish in response to vibrations was recorded for 3 min
474 immediately after the introduction of the vibration rod into the bowl. The vibration stimulus was
475 generated using a 7.5-mm diameter glass rod at 40 Hz with a GW Instek SFG-1003 DDS
476 Function Generator (Good Will Instrument Co., Ltd., New Taipei City, Taiwan) connected to an
477 audio speaker (ProSpeakers, Apple, Cupertino, CA, USA). Video footage of behavior was
478 recorded under infrared illumination (880-nm wavelength; BL41192-880 blacklight; Advanced
479 Illumination, Rochester, VT, USA) using a customized Microsoft MAIN-31891 LifeCam Studio
480 installed with a Zoom lens (Zoom 7000, Navitar, Rochester, NY) and VirtualDub2 video
481 capture software (licensed under the GNU General Public License:
482 https://sourceforge.net/projects/vdfiltermod/).
483 The NOA was analyzed using ImageJ macro plugins (ImageJ 1.53a; NIH, Bethesda, MD,
484 USA) and a homemade script published previously (Worsham et al., 2019; Yoshizawa et al.,

2010). Using this method, we measured NOA and selected Pachón cavefish that exhibited NOA ≥ 6 for the ablation study (see “Ablation experiments” below).

VAB video analysis using DLC

Videos were analyzed using the DLC toolbox version 2.0.6 (Mathis et al., 2018; Nath et al., 2019) in Python 3.6. DLC provides a robust suite of tools for deep learning-based markerless pose estimation. The approach is based on transfer learning, wherein a deep neural network is initially trained on an initial task with large amounts of available training data to achieve robust initial parameterization and then fine-tuned on a target task (ideally as closely related to the initial task as possible; in this case, pose estimation) using a smaller dataset. DLC uses a ResNet50 (He et al., 2016) backbone pretrained on the ImageNet (Deng et al., 2009) dataset to classify 1000 object categories in a dataset of over one million hand-labeled images. This network parameterization is then transferred and fine-tuned, during which the last layer of the network used originally for classification is replaced with transposed convolutional layers for pose estimation. These new layers predict individual probability densities over all pixels of a given input image for each pose marker, and such predictions are repeated independently for each frame in the video. DLC was also used to simplify data selection, data labeling, training, evaluation, and retraining processes. In this study, we specified a pose estimation task to track both the fish and rods in the VAB videos. For the fish, three head markers were tracked (right-side, left-side, and center) as well as one marker in the caudal fin; additionally, one marker was placed in the center of the vibrating rod. Because some videos contained two Petri dishes and some contained one, two separate sets of the same markers were allocated. The initial training set included frames selected randomly from 88 different VAB videos, and 807 hand-labeled training frames (images) were used to train our final model. The ResNet50 model was fine-tuned until the DLC early-stopping criterion was reached while using the default DLC training parameters as described by Mathis et al. (2018). All weights in the network were adjusted during training. The trained model was used to predict marker locations in all videos, outputting the x and y coordinates associated with the highest probability pixel for each marker. In frames with at least one DLC marker below a predefined confidence threshold, all marker locations were interpolated based on the markers’ positions in the preceding and following frames, which ensured that fish tracking was smooth throughout the duration of each video. Specifically, for a sequence of one or more subsequent frames where each frame had at least one marker below the confidence threshold, all markers’ locations were linearly

518 interpolated between each of the respective markers' locations in the frame immediately
519 preceding and the frame immediately following that sequence. For videos including multiple
520 recording arenas, markers for each Petri dish were treated independently. The confidence
521 threshold was set empirically to 0.92 after manual inspection of the DLC outputs. The resulting
522 marker locations were used to track several behaviors of interest in the videos: time spent
523 within a 1.3-cm radius of the rod (DIR), time spent being outside of this radius (DOR), left- and
524 right-sided approaches (NOA), and total swimming distance. The 1.3-cm radius from the
525 vibrating rod was determined as the cutoff of VAB because it was the distance that best
526 discriminated between the surface fish and cavefish approaches across the tested radii of 0.5–
527 2.5 cm (in 0.1-cm increments) from the vibrating rod. A left-sided approach was defined as
528 entering the 1.3-cm radius threshold with the head-center marker while the head-left marker
529 was closer than the head-right marker to the rod, and vice versa for a right-sided approach
530 (Figure 3A). Accordingly, DIR, DOR, and NOA were separated as right- or left-facing based on
531 the proximity of the head-right and head-left markers to the rod (Figure 3A).
532
533 **Repeatablity test**
534 Repeatablity test was performed as described previously (Yoshizawa et al., 2010). Briefly, we
535 first acclimated 22 surface, 9 Pachón cave and 11 Tinaja cave fish in cylindrical chambers for
536 4–5 days. Fish were fed once per day *ad libitum* with live *A. salina* larvae and recorded their
537 movement as described in the Recording VAB section. After the recording, the cylindrical
538 chambers were cleaned and fish were maintained in the same chambers for 6 days, and
539 rerecorded in 7th days of the second acclimation (6 days a part). This procedure was repeated
540 for the 3rd recording. The conditioned water was replaced every two days during this period.
541 After the behavior analysis using DLC, interclass correlation repeatability (3 repeated
542 measurements) was tested as referring Single_random_raters by the 'psych' R package.
543
544 **SN imaging**
545 Neuromast vital staining was performed as described previously (Jørgenson and Jørgensen,
546 1989; Worsham et al., 2019; Yoshizawa et al., 2010). Fish were immersed in 25 μg/mL of 4-(4-
547 (dimethylaminostyryl)−1-methylpyridiniumiodide (4-Di-1-ASP; MilliporeSigma, Burlington, MA)
548 dissolved in conditioned water for 40–60 min, after which they were anesthetized in 66.7
549 μg/mL of ice-cold ethyl 3-aminobenzoate methanesulfonate salt (MS222; MilliporeSigma) in
550 conditioned water (pH 6.8–7.0; conductivity of ~700 μS). Fish were then visualized using a

551 fluorescence microscope [BX61WI Olympus microscope with a 2.5× MPlanFL N lens, a
552 Rhodamine filter set, and an ORCA-Flash 4.0 digital camera (Olympus Corp.)]. SNs were
553 counted from digital images of 4-Di-1-ASP-stained fish using the "Analyze Particles" function of
554 ImageJ 1.53a. SNs were counted both in the left and right sides of the third
555 infraorbital/suborbital bone.
556
557 **Ablation experiments**
558 Ablation experiments were performed using 1-year old surface fish (n = 47) and VAB-positive
559 cavefish (Pachón population, n = 67). The VAB level was measured before ablation, and VAB-
560 positive cavefish (NOA ≥ 6 according to ImageJ-based analysis) were selected strategically to
561 determine the association between IO3 SNs and VAB level.
562 SN ablations were performed using Vetbond (3M, St. Paul, MN, USA), a nontoxic tissue
563 adhesive, on the left (surface fish, n = 14; Pachón cavefish, n = 30), right (surface fish, n = 13;
564 Pachón cavefish, n = 25), and both left and right (surface fish, n = 10; Pachón cavefish, n = 12)
565 sides (Figure 2A and B). Fish were anesthetized in 66.7 μg/mL of ice-cold ethyl 3-
566 aminobenzoate methanesulfonate salt (MS222, MilliporeSigma) in conditioned water (pH 6.8–
567 7.0; conductivity of ~700 μS). Excess water was removed carefully using Kimtech wipes, and
568 the adhesive (0.5 μL) was applied to the skin surface. After being exposed to the air for 10 s,
569 treated fish were placed in bowls (10 cm in diameter; 5 cm in height; Pyrex 325 mL, Corning)
570 filled with conditioned water at room temperature. Within a day of active swimming, the
571 adhesive usually peeled off, and VAB was assayed. 4-Di-1-ASP staining was performed to
572 count the number of SNs in the IO3 region before and after ablation.
573
574 **Fasting**
575 Pachón cavefish (n = 20), Tinaja cavefish (n = 20) and surface fish (n = 16) individuals (~1
576 year old) were placed in cylindrical chambers (10 cm in diameter; 5 cm in height; Pyrex 325
577 mL, Corning) and acclimated for 4–5 days in conditioned water (pH 6.8–7.0; conductivity of
578 ~600 μS) in which they were fed once a day (weight or approximate number of *Artemia*) with
579 live *A. salina* larvae. After acclimation, VAB was recorded and analyzed. Following this first
580 assessment, fish were starved for 6 days and VAB was recorded and analyzed once again.
581
582 **Statistical analysis**

All statistical analyses were performed in RStudio 4.0.3 (RStudio, Boston, MA, USA). The R packages used included lme4, lmerTest, car, coin, yarrr, AICcmodavg, and ggpubr. Linear or generalized linear models were selected using Akaike's information criterion function to identify the best fit models for analysis of the NOA and DIR in all experiments. Analysis of variance (ANOVA) was performed using generalized linear model fitting functions (glm or glmer in the lme4 package). Post-hoc tests were performed using the Wilcoxon signed-rank (paired) test followed by Holm's multiple-test correction. Nonparametric Kendall's t correlation was used to evaluate associations between neuromasts and behavior outputs. In the field experiments, the total number of turns within the circle were pooled for each cave pool, and the left-side turns vs. the right-side turns were tested by fitting a generalized linear mixed-effects model using a binomial distribution.

References

Aspiras AC, Rohner N, Martineau B, Borowsky RL, Tabin CJ. 2015. Melanocortin 4 receptor mutations contribute to the adaptation of cavefish to nutrient-poor conditions. *Proc Natl Acad Sci U S A* **112**:9668–9673. doi:10.1073/pnas.1510802112

Bisazza A, Cantalupo C, Capocchiano M, Vallortigara G. 2000. Population lateralisation and social behaviour: A study with 16 species of fish. *Laterality Asymmetries Body, Brain Cogn* **5**:269–284. doi:10.1080/713754381

Bisazza A, Dadda M. 2005. Enhanced schooling performance in lateralized fishes. *Proc R Soc B Biol Sci* **272**:1677–1681. doi:10.1098/rspb.2005.3145

Borowsky R. 2008. Restoring sight in blind cavefish. *Curr Biol* **18**:R23–R24.

Braun CB, Sand O. 2013. Functional Overlap and Nonoverlap Between Lateral Line and Auditory Systems In: Coombs S, Bleckmann H, Fay RR, Popper AN, editors. The Lateral Line System. Springer Handbook of Auditory Research 48. New York: Springer New York. pp. 281–312. doi:10.1007/2506_2013_19

Chivers DP, McCormick MI, Allan BJM, Mitchell MD, Gonçalves EJ, Bryshun R, Ferrari MCO. 2016. At odds with the group: changes in lateralization and escape performance reveal conformity and conflict in fish schools. *Proceedings Biol Sci* **283**:20161127. doi:10.1098/rspb.2016.1127

Chivers DP, McCormick MI, Warren DT, Allan BJM, Ramasamy RA, Arvizu BK, Glue M, Ferrari MCO. 2017. Competitive superiority versus predation savvy: the two sides of behavioural lateralization. *Anim Behav* **130**:9–15. doi:10.1016/J.ANBEHAV.2017.05.006

Culver DC. 1982. Cave life, evolution and ecology. Cambridge: Harvard University Press.

Culver DC, Pipan T. 2009. The biology of caves and other subterranean habitats, The biology of habitats series. Oxford: Oxford University Press.

Dadda M, Koolhaas WH, Domenici P. 2010. Behavioural asymmetry affects escape performance in a teleost fish. *Biol Lett* **6**:414–417. doi:10.1098/rsbl.2009.0904

de Perera TB, Braithwaite VAA, Burt de Perera T, Braithwaite VAA. 2005. Laterality in a non-visual sensory modality - the lateral line of fish. *Curr Biol* **15**:R241–R242. doi:10.1016/j.cub.2005.03.035

Deng J, Dong W, Socher R, Li L-J, Li K, Fei-Fei L. 2009. Imagenet: A large-scale hierarchical image database2009 IEEE Conference on Computer Vision and Pattern Recognition. pp. 248–255.

Espinasa L, Bonaroti N, Wong J, Pottin K, Queinnec E, Rétaux S. 2017. Contrasting feeding habits of post-larval and adult *Astyanax* cavefish. *Subterr Biol* **21**:1–17. doi:10.3897/subtbiol.21.11046

Espinasa L, Heintz C, Rétaux S, Yoshisawa M, Agnès F, Ornelas-Garcia P, Balogh-Robinson R. 2021. Vibration attraction response is a plastic trait in blind Mexican tetra (*Astyanax mexicanus*), variable within subpopulations inhabiting the same cave. *J Fish Biol* **98**:304–316. doi:10.1111/jfb.14586

Espinasa L, Ornelas-García CP, Legendre L, Rétaux S, Best A, Gamboa-Miranda R, Espinosa-Pérez H, Sprouse P. 2020. Discovery of Two New Astyanax Cavefish Localities Leads to Further Understanding of the Species Biogeography. *Diversity* **12**:368. doi:10.3390/d12100368

Fernandes VFL, Macaspac C, Lu L, Yoshizawa M. 2018. Evolution of the developmental plasticity and a coupling between left mechanosensory neuromasts and an adaptive foraging behavior. *Dev Biol* **441**:262–271. doi:10.1016/j.ydbio.2018.05.012

Fumey J, Hinaux H, Noirot C, Thermes C, Rétaux S, Casane D. 2018. Evidence for late Pleistocene origin of Astyanax mexicanus cavefish. *BMC Evol Biol* **18**:43.

doi:10.1186/s12862-018-1156-7
Gross JB, Gangidine A, Powers AK. 2016. Asymmetric facial bone fragmentation mirrors asymmetric distribution of cranial neuromasts in blind Mexican cavefish. *Symmetry (Basel)* **8**. doi:10.3390/sym8110118
Gross JB, Powers AK. 2016. The Evolution of the Cavefish Craniofacial Complex In: Keene AC, Yoshizawa M, McGaugh SE, editors. Biology and Evolution of the Mexican Cavefish. Amsterdam: Academic Press. pp. 193–207. doi:10.1016/B978-0-12-802148-4.00010-4
Güntürkün O, Ströckens F, Ocklenburg S. 2020. Brain Lateralization: A Comparative Perspective. *Physiol Rev* **100**:1019–1063. doi:10.1152/physrev.00006.2019
He K, Zhang X, Ren S, Sun J. 2016. Deep Residual Learning for Image RecognitionProceedings of the IEEE Conference on Computer Vision and Pattern Recognition (CVPR).
Heilman KM, Abell TVD. 1980. Right hemisphere dominance for attention: The mechanism underlying hemispheric asymmetries of inattention (neglect). *Neurology* **30**:327–327. doi:10.1212/WNL.30.3.327
Herman A, Brandvain Y, Weagley J, Jeffery WR, Keene AC, Kono TJY, Bilandžija H, Borowsky R, Espinasa L, O'Quin K, Ornelas-García CP, Yoshizawa M, Carlson B, Maldonado E, Gross JB, Cartwright RA, Rohner N, Warren WC, McGaugh SE. 2018. The role of gene flow in rapid and repeated evolution of cave-related traits in Mexican tetra, Astyanax mexicanus. *Mol Ecol* **27**:4397–4416. doi:10.1111/mec.14877
Jørgenson JM, Jørgensen JM. 1989. Evolution of octavolateralis sensory cells In: Coombs S, Görner P, Münz H, editors. The Mechanosensory Lateral Line. New York: Springer-Verlag. pp. 115–145.
Kalmijn AJ. 1988. Hydrodynamic and Acoustic Field DetectionSensory Biology of Aquatic Animals. New York, NY: Springer New York. pp. 83–130. doi:10.1007/978-1-4612-3714-3_4
Keene AC, Yoshizawa M, McGaugh SE. 2016. Biology and Evolution of the Mexican Cavefish, Biology and Evolution of the Mexican Cavefish. Amsterdam: Elsevier Inc. doi:10.1016/C2014-0-01426-8
Kohashi T, Nakata N, Oda Y. 2012. Effective sensory modality activating an escape triggering neuron switches during early development in zebrafish. *J Neurosci* **32**:5810–5820. doi:10.1523/JNEUROSCI.6169-11.2012
Landis JR, Koch GG. 1977. The measurement of observer agreement for categorical data. *Biometrics* **33**:159–74.
Lang HH. 1980. Surface wave discrimination between prey and nonprey by the back swimmerNotonecta glauca L. (Hemiptera, Heteroptera). *Behav Ecol Sociobiol* **6**:233–246. doi:10.1007/BF00569205
Magat M, Brown C. 2009. Laterality enhances cognition in Australian parrots. *Proc R Soc B Biol Sci* **276**:4155–4162. doi:10.1098/rspb.2009.1397
Mathis A, Mamidanna P, Cury KM, Abe T, Murthy VN, Mathis MW, Bethge M. 2018. DeepLabCut: markerless pose estimation of user-defined body parts with deep learning. *Nat Neurosci* **21**:1281–1289. doi:10.1038/s41593-018-0209-y
Mitchell RW, Russell WH, Elliott WR. 1977. Mexican eyeless characin fishes, genus Astyanax: Environment, distribution, and evolution., Special pu. ed, Special publications the museum Texas Tech University. Texas: Texas Tech Press.
Montgomery JC, Macdonald JA. 1987. Sensory Tuning of Lateral Line Receptors in Antarctic Fish to the Movements of Planktonic Prey Published by : American Association for the Advancement of Science Stable URL : https://www.jstor.org/stable/1698962 **235**:195–196.
Nath T, Mathis A, Chen AC, Patel A, Bethge M, Mathis MW. 2019. Using {DeepLabCut} for

{3D} markerless pose estimation across species and behaviors. *Nat Protoc* **14**:2152–2176. doi:10.1038/s41596-019-0176-0

Neumann S, Doubell TP, Leslie T, Woolf CJ. 1996. Inflammatory pain hypersensitivity mediated by phenotypic switch in myelinated primary sensory neurons. *Nature* **384**:360–364. doi:10.1038/384360a0

Nottebohm F. 1977. Asymmetries in neural control of vocalization in the canary In" Lateralization of the Nervous System"(S. Harnard, ed.).

Nottebohm F. 1971. Neural lateralization of vocal control in a passerine bird. I. Song. *J Exp Zool* **177**:229–261. doi:10.1002/jez.1401770210

Nottebohm F, Nottebohm ME. 1976. Left hypoglossal dominance in the control of canary and white-crowned sparrow song. *J Comp Physiol ■ A* **108**:171–192. doi:10.1007/BF02169047

Ornelas-García C, Domínguez-Domínguez O, Doadrio I. 2008. Evolutionary history of the fish genus Astyanax Baird & Girard (1854) (Actinopterygii, Characidae) in Mesoamerica reveals multiple morphological homoplasies. *BMC Evol Biol* **8**:340. doi:10.1186/1471-2148-8-340

Popper AN, Fay RR. 2011. Rethinking sound detection by fishes. *Hear Res* **273**:25–36. doi:10.1016/j.heares.2009.12.023

Powers AK, Davis EM, Kaplan SA, Gross JB. 2017. Cranial asymmetry arises later in the life history of the blind Mexican cavefish, Astyanax mexicanus. *PLoS One* **12**:e0177419. doi:10.1371/journal.pone.0177419

Protas M, Jeffery WR. 2012. Evolution and development in cave animals: from fish to crustaceans. *Wiley Interdiscip Rev Dev Biol* **1**:823–845. doi:10.1002/wdev.61

Rétaux S, Casane D, Rétaux S, Casane D. 2013. Evolution of eye development in the darkness of caves: adaptation, drift, or both? *Evodevo* **4**:26.

Rogers LJ. 1989. eScholarship International Journal of Comparative Psychology Title Laterality in Animals Permalink Publication Date. *Int J Comp Psychol* **3**.

Rogers LJ. 1981. Environmental influences on brain lateralization. *Behav Brain Sci* **4**:35–36.

Rogers LJ, Workman L. 1989. Light exposure during incubation affects competitive behaviour in domestic chicks. *Appl Anim Behav Sci* **23**:187–198. doi:10.1016/0168-1591(89)90109-3

Schwartz G, Davidson R, Maer F. 1975. Right hemisphere lateralization for emotion in the human brain: interactions with cognition. *Science (80-)* **190**:286–288. doi:10.1126/science.1179210

Sovrano VA, Dadda M, Bisazza A. 2005. Lateralized fish perform better than nonlateralized fish in spatial reorientation tasks. *Behav Brain Res* **163**:122–7. doi:10.1016/j.bbr.2005.04.012

Strecker U, Hausdorf B, Wilkens H. 2012. Parallel speciation in Astyanax cave fish (Teleostei) in Northern Mexico. *Mol Phylogenet Evol* **62**:62–70.

Tommasi L. 2009. Mechanisms and functions of brain and behavioural asymmetries. *Philos Trans R Soc Lond B Biol Sci* **364**:855–9. doi:10.1098/rstb.2008.0293

Tricas TCTC. 2020. Acoustic Ecology, Communication and Peripheral Signal Processing in Fishes. In: Fritzsch B, Grothe B, editors. The Senses: A Comprehensive Reference, Vol. 2. Cambridge: Academic Press. pp. 114–137. doi:10.1016/B978-0-12-809324-5.24220-X

Wang H, Dai Y, Fukuoka T, Yamanaka H, Obata K, Tokunaga A, Noguchi K. 2004. Enhancement of stimulation-induced ERK activation in the spinal dorsal horn and gracile nucleus neurons in rats with peripheral nerve injury. *Eur J Neurosci* **19**:884–890. doi:10.1111/j.0953-816X.2004.03203.x

Wernicke C. 1874. Der aphasische Symptomencomplex: eine psychologische Studie auf anatomischer Basis. Cohn.

Wilkens H, Hecht MK, Wallace B, Wilkens H. 1988. Evolution and genetics of epigean and

cave Astyanax-fasciatus (Characidae, Pisces) - Support for the neutral mutation theory In: Hecht M K, Wallace B, editors. Evolutionary Biology. New York: Plenum Publishing Corporation. pp. 271–367. doi:10.1007/978-1-4613-1043-3_8

Wilson EV V, Thomas RQQ, Evans LMM. 2004. Macrobrachium as a possible determinant of *Astyanax fasciatus* distribution in a neotropical lowland stream. *Dartmouth Stud Trop Ecol* **2004**:99–102.

Worsham M, Lima Fernandes VF, Settle A, Balaan C, Lactaoen K, Tuttle LJ, Iwashita M, Yoshizawa M. 2019. Behavioral tracking and neuromast imaging of Mexican cavefish. *J Vis Exp* **2019**. doi:10.3791/59099

Yoshizawa M. 2015. Behaviors of cavefish offer insight into developmental evolution. *Mol Reprod Dev* **82**:268–280. doi:10.1002/mrd.22471

Yoshizawa M, Ashida G, Jeffery WR. 2012a. Parental genetic effects in a cavefish adaptive behavior explain disparity between nuclear and mitochondrial DNA. *Evolution (N Y)* **66**:2975–2982. doi:10.1111/j.1558-5646.2012.01651.x

Yoshizawa M, Gorički S, Soares D, Jeffery WR. 2010. Evolution of a behavioral shift mediated by superficial neuromasts helps cavefish find food in darkness. *Curr Biol* **20**:1631–1636. doi:10.1016/j.cub.2010.07.017

Yoshizawa M, Jeffery WR. 2011. Evolutionary tuning of an adaptive behavior requires enhancement of the neuromast sensory system. *Commun Integr Biol* **4**:89–91. doi:10.1016/j.cub.2010.0

Yoshizawa M, Robinson BG, Duboué ER, Masek P, Jaggard JB, O'Quin KE, Borowsky RL, Jeffery WR, Keene AC. 2015. Distinct genetic architecture underlies the emergence of sleep loss and prey-seeking behavior in the Mexican cavefish. *BMC Biol* **13**:15. doi:10.1186/s12915-015-0119-3

Yoshizawa M, Yamamoto Y, O'Quin KE, Jeffery WR. 2012b. Evolution of an adaptive behavior and its sensory receptors promotes eye regression in blind cavefish. *BMC Biol* **10**:108. doi:10.1186/1741-7007-11-82

Zegers M, de Bruijne MC, Wagner C, Groenewegen PP, van der Wal G, de Vet HCW. 2010. The inter-rater agreement of retrospective assessments of adverse events does not improve with two reviewers per patient record. *J Clin Epidemiol* **63**:94–102. doi:10.1016/j.jclinepi.2009.03.004

Figures

Figure 1

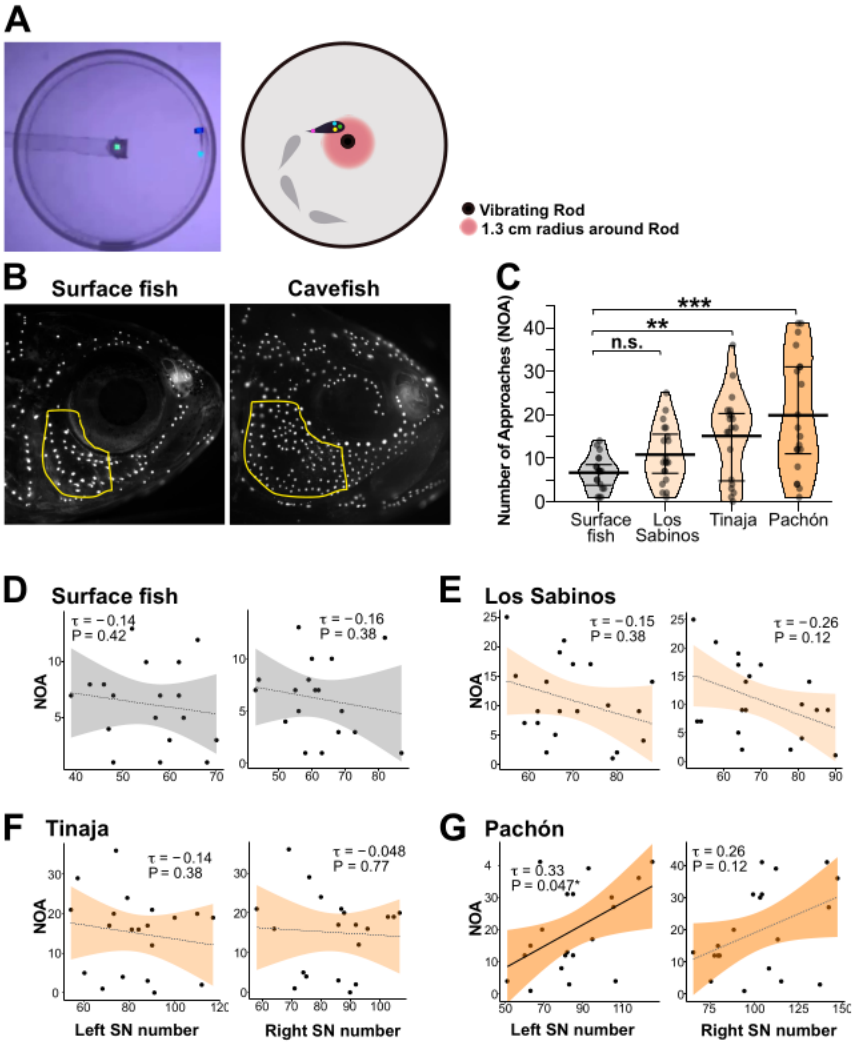

Figure 1. Sensory laterality in surface fish and cavefish populations of *Astyanax mexicanus*. VAB videos were analyzed using a home-developed Python script and a DeepLabCut deep learning algorithm. This method allowed us to detect the number of times fish made left or right approaches toward the vibrating rod (NOA) and the associated duration they spent within a 1.3-cm radius from the vibrating rod (DIR). (**A**) Video image (left) and schematic representation (right) of fish and the vibrating rod labeled with three markers on the head (left, center, and right) and one marker on the caudal fin. (**B**) Superficial neuromasts (SNs) in the infraorbital region (IO3 region delimited by a yellow line) were stained with 4-Di-1-ASP vital dye. (**C**) NOA data for the lab-raised populations indicated that Pachón cavefish showed the highest NOA values. The bars in the pirate plots represent means ± standard errors of the means (each population, n = 20). *, $P < 0.05$; **, $P < 0.01$; and ***, $P < 0.001$. Statistical scores are shown in Supplementary Table 1. (**D–G**) The number of SNs in the left or right IO3 area plotted against the total NOA in surface fish (**D**) and Los Sabinos (**E**), Tinaja (**F**), and Pachón cavefish (**G**). Statistical scores are available in Supplementary Table 2.

Figure 2

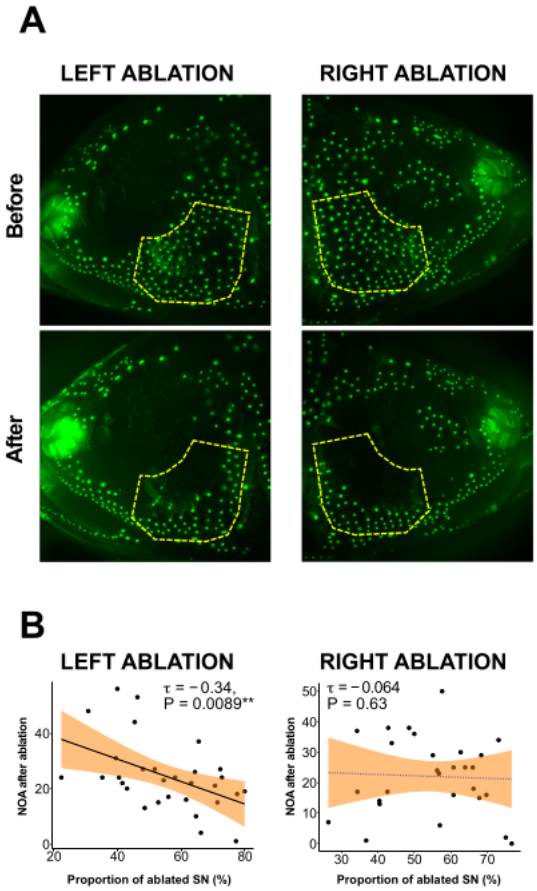

Figure 2. Ablation of superficial neuromasts (SNs) confirmed that the left-side SN promotes the level of VAB in Pachón cavefish. (**A**) Left and right sides of SNs in Pachón cavefish stained with 4-Di-1-ASP (green dots) before and after ablation of SNs in the infraorbital region (IO3 shown by a yellow line) of the same fish. (**B**) Proportion of ablated SNs on the left-side and right-side plotted against the total NOA in both cases. Regression lines with 95% confidence intervals (shaded gray or orange) are shown in each panel. See Supplementary Table 3 for additional details. **, $P < 0.01$.

Figure 2--figure supplement 1

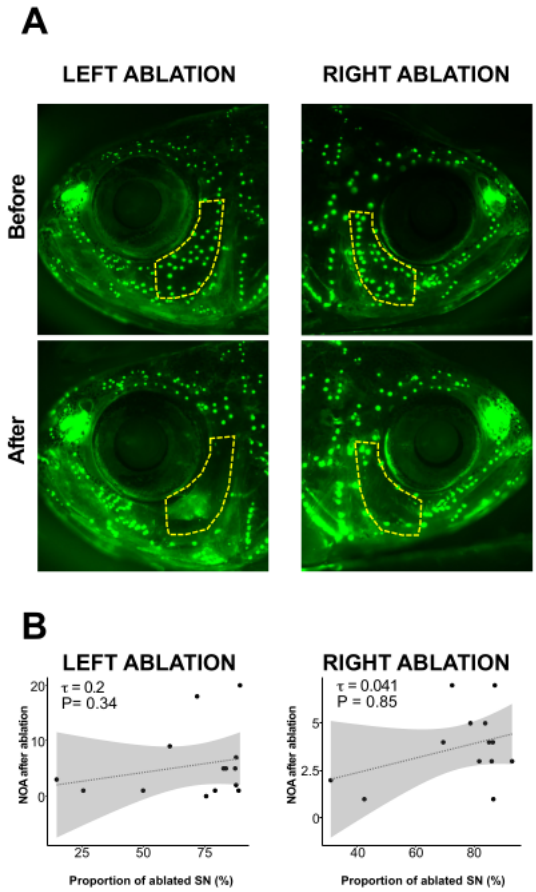

Figure 2—figure supplement 1. Ablation of superficial neuromasts (SNs) did not induce detectable effect on the level of VAB in surface fish. (**A**) Left and right sides of SNs in Pachón cavefish stained with 4-Di-1-ASP (green dots) before and after ablation of SNs in the infraorbital region (IO3 shown by a yellow line) of the same fish. (**B**) Proportion of ablated SNs on the left and right sides plotted against the total NOA in both cases. Regression lines with 95% confidence intervals (shaded gray or orange) are shown in each panel. See Supplementary Table 3 for additional details.

Figure 2--figure supplement 2

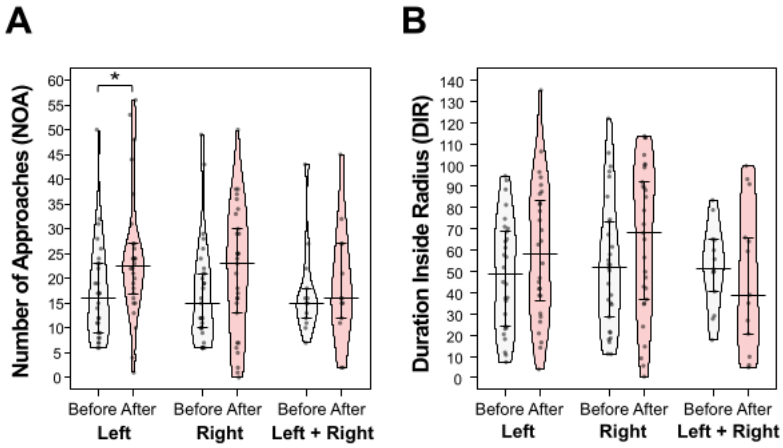

Figure 2—figure supplement 2. Overall results of the SN ablation experiments in Pachón cavefish. (**A**) Number of approaches (NOA) in Pachón cavefish. Ablation of the left SN resulted in an increase in NOA (V = 74.5, P = 0.032); however, ablation of the right SN changed NOA at an underdetection level (V = 121, P = 0.063). (**B**) Duratin in the radius (DIR) in Pachón cavefish. Left SN or right SN ablation did not show detectable changes in DIR. Pirate plot bars represent means ± standard errors of the means. Data were analyzed using a generalized linear model followed by a post-hoc test (Wilcoxon test, adjusted by Holm's correction): *, $P < 0.05$; **, $P < 0.01$; and ***, $P < 0.001$. Statistical scores are available in Supplementary Table 4.

Figure 3

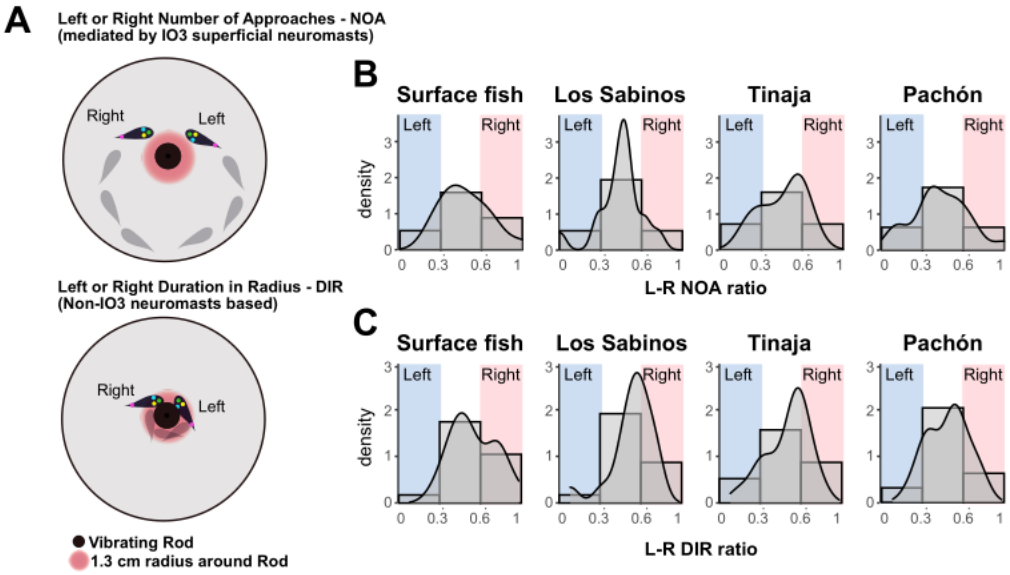

Figure 3. Laterality in behavioral output among surface fish and cavefish populations of *Astyanax mexicanus*. (**A**) Schemes representing left or right approaches expressed as NOA (top) and left or right adherence expressed as DIR (bottom). (**B**) Histograms for the L–R NOA ratio (the right-side NOA divided by the total NOA: $\frac{NOA(right)}{NOA(right)+NOA(left)}$) across all four populations. (**C**) Histograms for the L–R DIR ratio ($\frac{DIR(right)}{DIR(right)+DIR(left)}$) across all four populations. Ratios of <0.33 indicate a strong left preference, ratios of 0.33–0.67 indicate balanced approaches, and ratios of >0.67 indicate a strong right preference. Los Sabinos cavefish showed a gaussian-like distribution, whereas many surface fish and the other cavefish individulas exhibited strong left or right bias. Notably, all four populations included a few individuals that showed strong left or right preferences (near 0.0 or 1.0, respectively).

Figure 3--figure supplement 1

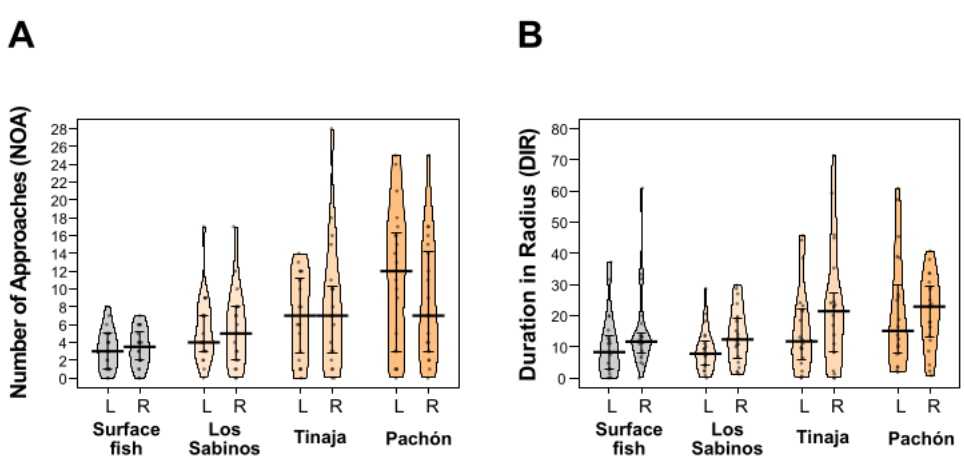

Figure 3—figure supplement 1. *Astyanax mexicanus* populations did not exhibit left- or right-biased approaches (NOA) or adhesion (DIR) at the population level.

843 (**A, B**) Pirate plots showing no detectable differences between the number of left- and right-
844 side approaches (NOA) (**A**) or the duration in the radius (DIR) (**B**) among the four tested
845 populations (2–3-year-old individuals). Data represent means ± standard errors of the means
846 (each population, n = 20). Further details are presented in Supplementary Table 1.
847

Figure 4

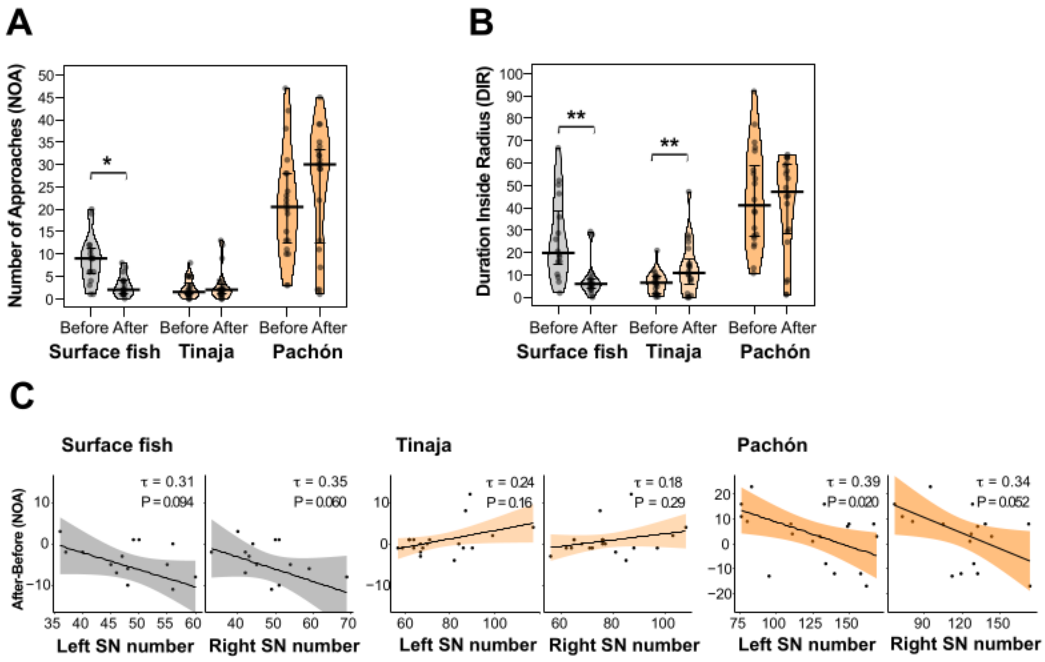

Figure 4. Plasticities of surface fish and Tinaja cavefish in total NOA and/or DIR, and the plastic left SN–NOA association in Pachón cavefish in response to fasting. (**A**) Pirate plots showing total NOA. Surface fish showed significantly reduced NOA after fasting, but neither Tinaja nor Pachón cavefish showed significant changes in NOA. (**B**) Pirate plots showing total DIR. Surface fish showed significantly reduced DIR after fasting, but Tinaja's DIR increased after fasting. Pachón cavefish showed no significant changes in DIR. (**C**) The number of left or right SNs plotted against changes in NOA after fasting (NOA_{after}–NOA_{before}) in surface fish, Tinaja cavefish, and Pachón cavefish. In Pachón cavefish, individuals with fewer left SNs showed a higher increase in total NOA, suggesting that a plastic response to fasting existed in individuals with few left SNs and a low NOA level. There was no detectable correlation between the number of right SNs and the change in NOA in Pachón cavefish or the other populations. All statistical scores are available in Supplementary Table 5 and 7.

Figure 5

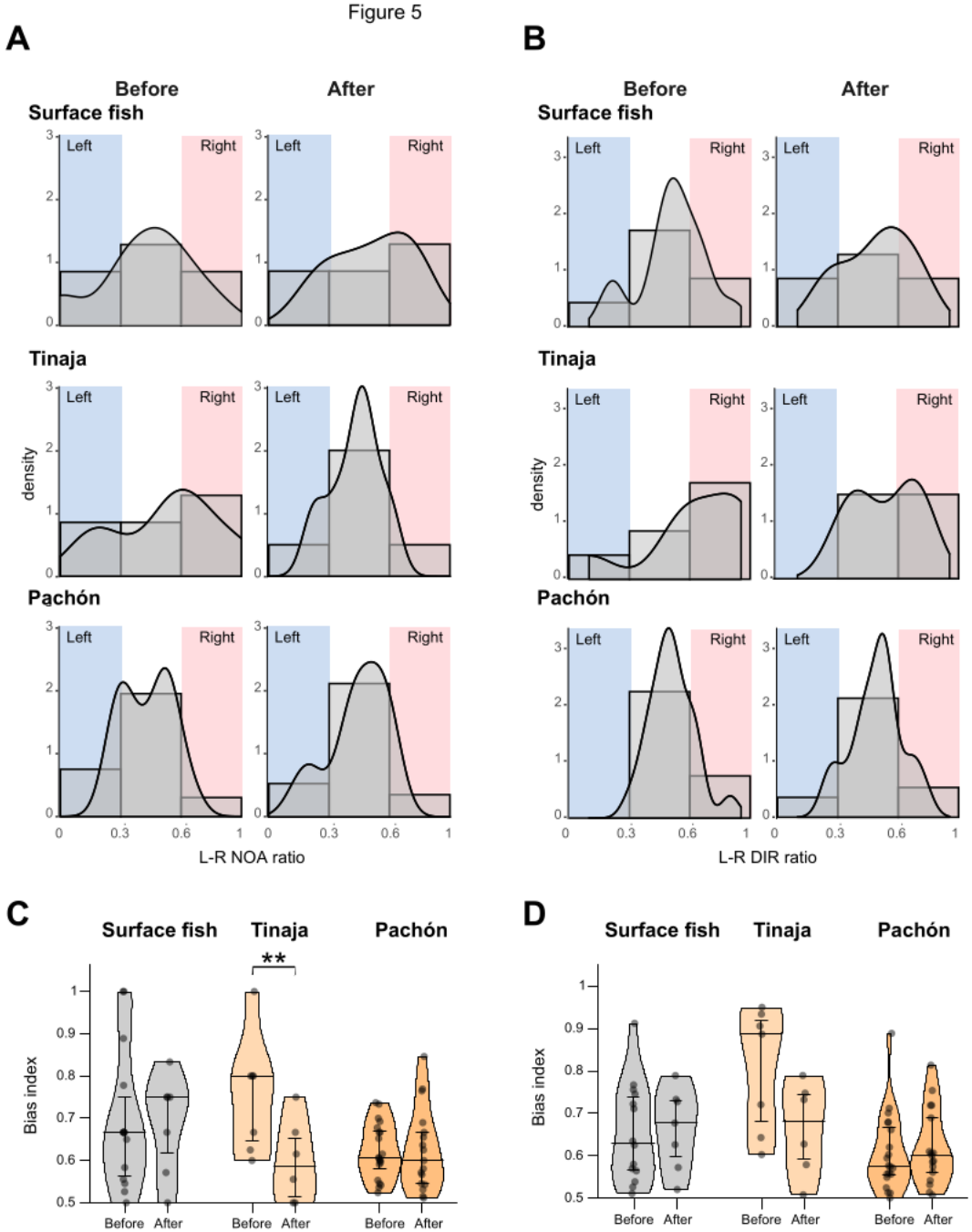

Figure 5. Right-biased approaches (NOA) in Tinaja cavefish were reduced after fasting. (**A, B**) Histograms and density plots showing the L–R NOA ratio (**A**) and L–R DIR ratio (**B**) before and after fasting in the indicated populations. In **A**, more Tinaja cavefish individuals showed L–R balanced approaches (0.33–0.67) after fasting; Pachón cavefish maintained L–R balanced approaches (0.33–0.67) before and after fasting, whereas surface fish showed a slight right bias. L–R NOA ratio = $\frac{NOA(right)}{NOA(right)+NOA(left)}$. In **B**, the trends for DIR were similar to those in (A). L–R DIR ratio = $\frac{DIR(right)}{DIR(right)+DIR(left)}$. (**C, D**) Pirate plots showing L–R bias index for NOA (**C**) and DIR (**D**). In **C**, Right bias index =$\frac{\max\{NOA(right),NOA(left)\}}{NOA(right)+NOA(left)}$. Tinaja cavefish showed a significantly reduced bias index for NOA after fasting, indicating balanced L–R approaches, whereas the other populations showed no detectable changes. In **D**, L–R bias index =

$\frac{\max\{DIR(right), DIR(left)\}}{DIR(right)+DIR(left)}$. None of the populations showed detectable changes in the bias index after fasting, although Tinaja cavefish showed a nonsignificant trend for reduced bias after fasting. All statistical scores are available in Supplementary Table 6. **, P < 0.01.

Figure 5--figure supplement 1

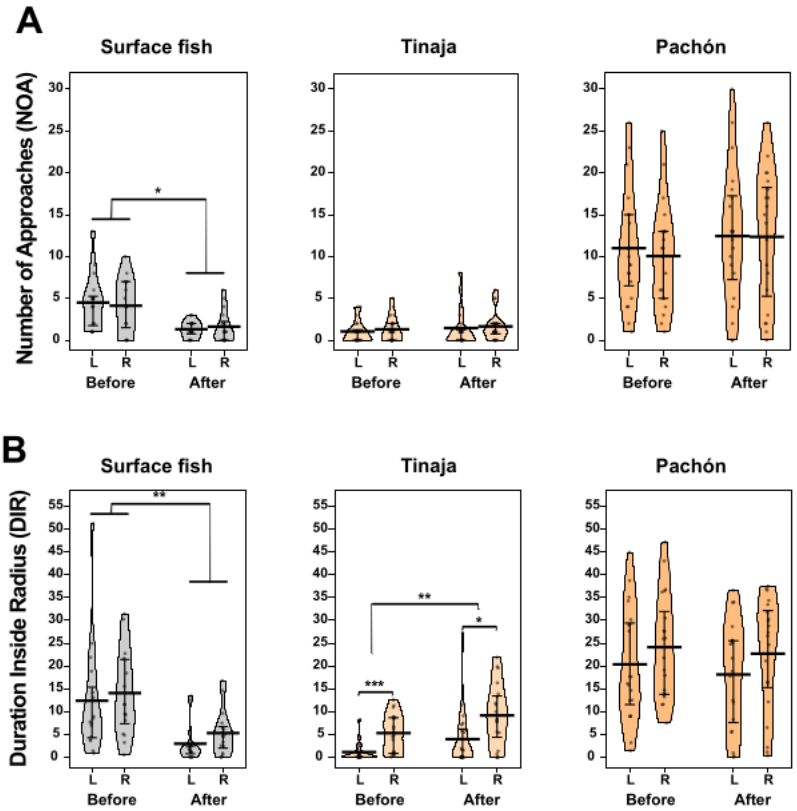

Figure 5—figure supplement 1. In response to starvation, lateralities in NOA and DIR are plastic in Tinaja cavefish but not in Pachón cavefish. (**A, B**) Pirate plots showing the number of left- and right-side approaches (NOA) (**A**) and left- and right-side-associated durations within a 1.3-cm radius (DIR) (**B**) before and after a 6-day fasting period. In **A**, only surface fish showed a significantly reduced NOA after fasting among the three tested populations, and no L–R bias (laterality) was detectable. In **B**, surface fish showed significantly reduced DIR after fasting, whereas Tinaja cavefish showed increased DIR after fasting. Tinaja cavefish also showed right bias in DIR before and after fasting, but they showed more significant right bias than left bias in DIR before fasting. Pachón cavefish did not exhibit any changes in DIR or L–R bias in DIR. All statistical scores are available in Supplementary Table 5. *, P < 0.05; **, P < 0.01.

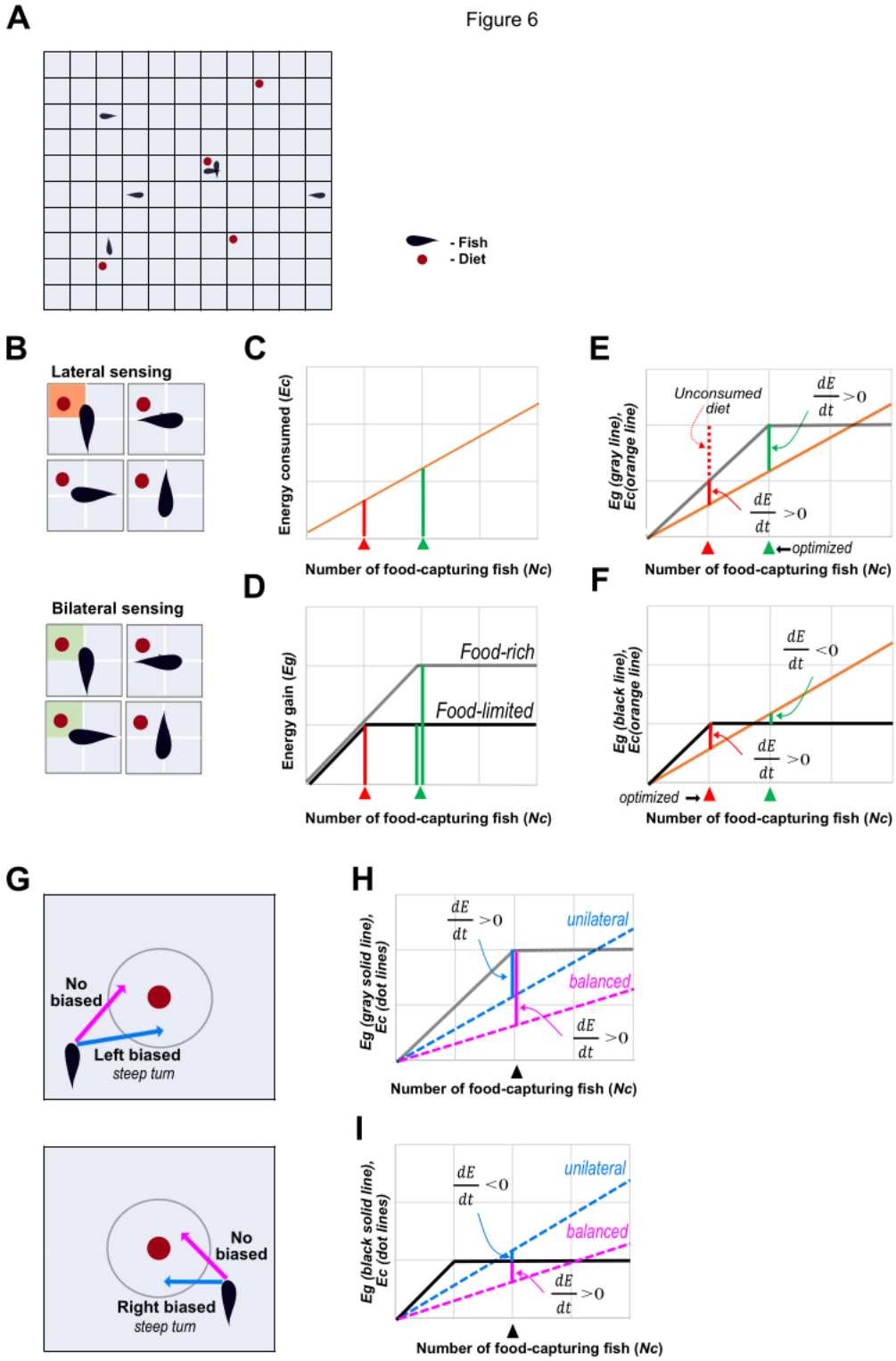

Figure 6. Relevance of sensory and behavior laterality. (**A**) General schematic of the model showing food availability and the number of fish. Each cell represents the sensing range of a fish. Red dots represent diet and black shapes represent fish. (**B**) In a given cell, the food detection probability p_d is 1/4 for lateral sensing (top) and 1/2 for bilateral sensing (bottom); red and green shaded areas represent overlapping areas in the food and sensing fields, respectively**.** (**C**) Energy consumption (E_c) as a function of the number of food-acquiring fish (N_c). (**D**) Energy gain from food (E_g) as a function of the number of food-acquiring fish (N_c). In **C** and **D**, red arrows and lines indicate lateral sensing fish and green arrows and lines indicate

bilateral sensing fish. Gray and black lines are the functions E_g and depend on food-rich and -limited conditions, respectively. (**E, F**) Evaluation of $\frac{dE}{dt}$. **E** shows E_g and E_c under food-rich conditions, whereas **F** shows E_g and E_c under food-limited conditions. $\frac{dE}{dt}$ is based on the subtraction of E_c from E_g and is shown as solid vertical lines (green and red). In **E** (food-rich condition), the bilateral population is optimized because $\frac{dE}{dt}$ of the bilateral sensing population is larger than that of the unilateral sensing population. Furthermore, there is no unconsumed food in the bilateral sensing population, whereas unconsumed food is present in the unilateral sensing population (red dotted line). In **F** (food-limited condition), the unilateral population is optimized because $\frac{dE}{dt}$ of the unilateral sensing population has a positive value, whereas $\frac{dE}{dt}$ in the bilateral sensing population is negative. (**G**) Food-approaching behavior. The gray circle shows the 1.3-cm radius from the food (red circle). Blue and pink arrows represent steeper and less steep turns, respectively. Fish with balanced approaches take either left or right approaches, whereas fish with biased approaches (laterality) always take one-sided approaches that frequently require steeper turns. (**H, I**) Evaluation of $\frac{dE}{dt}$ in food-rich (**H**) and food-limited (**I**) environments. The E_c values for unilateral (steeper turn) fish and balanced fish are shown as blue and pink dotted lines, respectively. $\frac{dE}{dt}$ is based on the subtraction of E_c (dotted lines) from E_g (gray solid line in H or black in I); therefore, it is expressed as the blue and pink vertical solid lines. Under food-rich conditions, $\frac{dE}{dt}$ for both unilateral and balanced fish is positive; thus, both populations can gain energy. In contrast, under food-limited conditions, the L–R balanced population is optimal because it shows a positive value for $\frac{dE}{dt}$. See Supplementary file 1 for further information.